Optica Applicata, Vol. XXI, No. 3, 1991

Optimization of reconstruction geometry for maximum diffraction efficiency in HOE — the influence of recording material*

A. BELÉNDEZ, I. PASCUAL, A. FIMIA

Laboratorio de Optica, Departamento Interuniversitario de Optica, Universidad de Alicante, Alicante 03080, Spain.

In this paper, the relation between recording and reconstruction geometries for maximum diffraction efficiency in thick holographic lenses is analysed. Theoretical expressions are presented when variations in recording material due to processing are taken into account. A particular holographic lens is studied in both theoretical as well as experimental terms, in order to find the optimized reconstruction geometry for maximum diffraction efficiency and the aberration that appears.

1. Introduction

Holographic optical elements (HOEs) are diffractive optical elements (DOEs), and therefore work by diffracting light from a generalized grating structure with nonuniform groove spacing [1]. This complex diffraction grating transforms the phase of an incoming wavefront into an output phase. To obtain HOEs with high diffraction efficiency, it is necessary to record these elements as thick phase holograms. It is possible to consider two important questions connected with the thick HOEs making [2]. The first is the design and analysis of the HOE, the second the recording material used to record the HOE. In order to quantify the performance of a HOE one can evaluate aberrations and diffraction efficiency.

As a result of the variations in recording material introduced by the chemical processing of the HOE, the reconstruction geometry corresponding to maximum diffraction efficiency has to be changed with respect to the recording geometry, which evidently gives rise to the appearance of aberrations in the HOE during the reconstruction stage [3], [4].

In this paper, we present matrix relations between the reconstruction and recording coordinates of the sources in a holographic lens (HL), when these changes appear in recording material due to chemical process, when recording and readout wavelengths are different and when Bragg's law is observed. According to this, and after introducing the experimental values of recording material variations due to

* This paper was presented at the International Colloquium on Diffractive Optical Elements DOE'91, May 14–17, 1991, Szklarska Poręba, Poland.

processing into the equation, it is possible to evaluate the aberrations in the reconstruction stage of HLs when diffraction efficiency is maximum. We present theoretical and experimental results in the optimization of reconstruction geometry of an HL for maximum diffraction efficiency and when recording and reconstruction wavelengths are identical. Also, we evaluate the aberrations introduced due to the changes between recording and reconstruction geometries, using a root mean square of wavefront aberration. In such a case, it is possible to find geometries in which the combinations of wavelengths and recording material changes create situations in which the aberrations are minimized and, at the same time, high diffraction efficiencies are achieved. This offers new opportunities in the field of HOE design in which the recording material plays an essential role.

2. Influence of recording material and its processing on the desired HOE

In the chemical processing of holographic recording material, used for making thick phase holograms, we use liquid solutions and, as a consequence, there is a change in the average refractive index and a deformation of the recording material. Due to the compensation of elastic forces during processing, there is a deformation of the volume material and a change in the interference fringes' orientation. As a result of these variations, the grating vector before processing is different from the recording grating vector. However, there is a change in the average refraction index of the material due to processing. As a result of all these variations, the reconstruction geometry for maximum diffraction efficiency will be different from the recording geometry.

For a holographic grating, the grating vector can be written as [5]

$$\boldsymbol{K} = \boldsymbol{k}_{\mathrm{R}}' - \boldsymbol{k}_{\mathrm{O}}' \tag{1}$$

where $\boldsymbol{k}_{\mathrm{R}}'$ and $\boldsymbol{k}_{\mathrm{O}}'$ are the propagation vectors of the reference (R) and object (O) beams in the medium of refractive index n_{R}, respectively. In order to study the influence of the process on a thick holographic grating, we have developed a geometrical model, i.e., the effective holographic grating model [6], [7]. Using this model, the relationships between the grating vectors $\boldsymbol{K}$ and $\boldsymbol{K}^*$ (before and after processing, respectively) are expressed as:

$$K_x^* = K_x, \tag{2}$$

$$K_z^* = \frac{1}{T_{\mathrm{e}}} K_z \tag{3}$$

where $T_{\mathrm{e}} = t_{\mathrm{e}}/t_{\mathrm{R}}$ (t_{e} is the "effective thickness" and t_{R} is the initial thickness of the medium, respectively). T_{e} is expressed as follows [7]:

$$T_{\mathrm{e}} = \frac{\tan\Phi}{\tan\delta + \tan\Phi} T \tag{4}$$

where $T = t_{\mathrm{C}}/t_{\mathrm{R}}$ (t_{C} is the thickness of the medium after processing), Φ is the angle

of Bragg plane inclination with respect to the Z axis and δ is the "cut" or "shear" angle, similar to those described in the theory of elasticity as can be seen in Fig. 1.

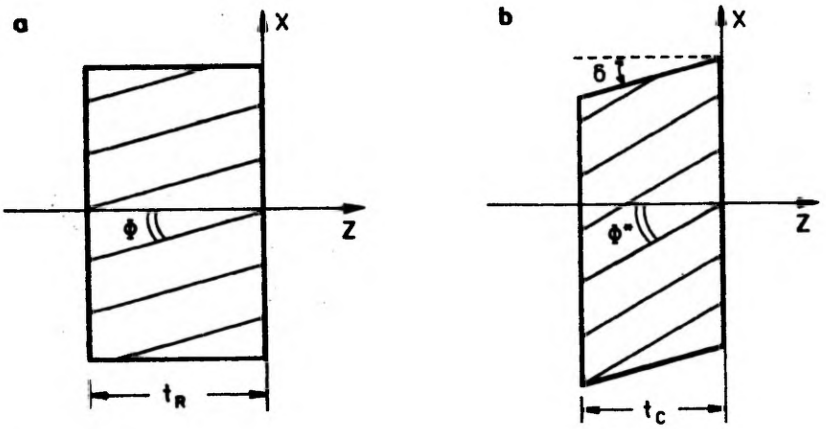

Fig. 1. Deformation of the holographic grating due to processing: (a) before processing, (b) after processing

This shear effect is due to the inclination of the Bragg planes and these δ angles will be small (only a few degrees).

After processing, Bragg's law can be written as

$$\boldsymbol{K}^* = \boldsymbol{k}'_C - \boldsymbol{k}'_I \tag{5}$$

where $\boldsymbol{k}'_C$ and $\boldsymbol{k}'_I$ are the propagation vectors of the reconstruction (C) and image (I) beams in the medium of refractive index n_C after processing.

The effective thickness plays a principal role in thick holographic gratings because it is directly related to the reconstruction angle which complies with Bragg's law. If this angle is α_C, the following equation can be obtained for transmission gratings by developing Eq. (5)

$$\sin\alpha_C = \frac{1}{2}\left[\frac{N}{T_e} + \mu\right] + \sin\alpha_R + \frac{1}{2}\left[\frac{N}{T_e} - \mu\right]\sin\alpha_O \tag{6}$$

where α_R and α_O are the recording angles of the grating, $N = n_C/n_R$ and $\mu = \lambda_C/\lambda_R$, λ_R and λ_C being the recording and the reconstruction wavelengths, respectively. It is possible to determine the T_e/N quotient experimentally by using

$$\frac{T_e}{N} = \frac{\sin\alpha_R + \sin\alpha_O}{2\sin\alpha_C + \mu(\sin\alpha_O - \sin\alpha_R)}. \tag{7}$$

In other words, the measurements of the reference α_R and object α_O angles and the reconstruction angle α_C in compliance with Bragg's law do not give the actual thickness but rather the effective thickness.

3. High-diffraction efficiency condition in the HOE

It is possible to apply the relationship presented in the previous section to holographic lenses using an approximation of the local grating [8], which produces a set of relationships between the coordinates of the recording and reconstruction sources when spherical and collimated wavefronts are used and Bragg's law is complied with in the reconstruction stage.

Figure 2 shows the geometry used for the analysis of holographic lenses. The HL is located in the XY plane, and the origin $Q(x_q, y_q, z_q)$ of a wavefront is defined in terms of the parameters R_q, α_q and β_q, where $q = \mathrm{R}, \mathrm{O}, \mathrm{C}, \mathrm{I}$. The sign of R_q is chosen such as to be equivalent to the sign of the corresponding coordinate z_q [3].

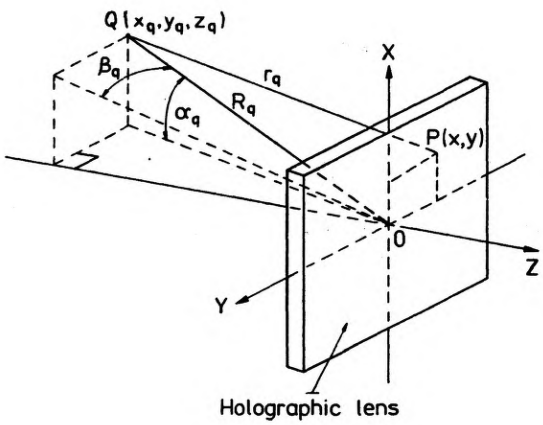

Fig. 2. Geometry for recording and reconstruction of the holographic lens. $Q(x_q, y_q, z_q)$ (with $q = \mathrm{R}, \mathrm{O}, \mathrm{C}, \mathrm{I}$) is an arbitrary point source situated in the XYZ space in front of a HL in the XY plane

During the recording of the HL, over any (x, y) point of the HL surface we will have the wave propagation vectors $\boldsymbol{k}_{\mathrm{R}}(x, y, 0)$ and $\boldsymbol{k}_{\mathrm{O}}(x, y, 0)$, that inside the holographic recording material of refractive index n_{R} will be $\boldsymbol{k}'_{\mathrm{R}}(x, y, 0)$ and $\boldsymbol{k}'_{\mathrm{O}}(x, y, 0)$. Using the approximation of the local grating over any small region of the HL, the interference pattern approximates a plane grating. Since the components of the propagation vectors will not vary significantly as a function of the z coordinate inside the recording material [9], and since we can evaluate these vectors at the plane $Z = 0^+$; i.e., propagation vectors inside the recording material are $\boldsymbol{k}'_{\mathrm{R}}(x, y, 0^+) \equiv \boldsymbol{k}'_{\mathrm{R}}(x, y)$ and $\boldsymbol{k}'_{\mathrm{O}}(x, y, 0^+) \equiv \boldsymbol{k}'_{\mathrm{O}}(x, y)$.

The interference pattern looks locally like a plane grating of a grating vector

$$\boldsymbol{K}(x, y) = \boldsymbol{k}_{\mathrm{R}}(x, y) - \boldsymbol{k}'_{\mathrm{O}}(x, y). \tag{8}$$

The z component of the propagation vector $\boldsymbol{k}'_q(x, y)$, k'_{qz}, can be derived from x and y components, k'_{qx} and k'_{qy}, yielding

$$k'_{qz} = \sqrt{\left(\frac{2\pi n_q}{\lambda_q}\right)^2 - k'^2_{qx} - k'^2_{qy}}. \tag{9}$$

After the HL processing and in order to obtain high-diffraction efficiency, it is necessary to fulfill the Bragg condition given by

$$\boldsymbol{K}^*(x, y) = \pm[\boldsymbol{k}'_C(x, y) - \boldsymbol{k}'_1(x, y)]. \tag{10}$$

In this equation, the $\pm$ sign refers to the use of the $+1$ diffracted order $(+)$ or -1 diffracted order $(-)$ of the holographic lens.

Taking into account Equations (2), (3), the components of the grating vectors $\boldsymbol{K}$ and $\boldsymbol{K}^*$ (before and after processing) are expressed by the following equations:

$$K^*_x(x, y) = K_x(x, y), \tag{11}$$

$$K^*_y(x, y) = K_y(x, y), \tag{12}$$

$$K^*_z(x, y) = [1/T_e(x, y)]K_z(x, y). \tag{13}$$

Now, the T_e parameter will be different for any local grating and will be a function of any (x, y) point of the HL surface. Substituting Eq. (8) and (10) into Eqs. (11)–(13), we obtain the equations:

$$k'_{Cx}(x, y) - k'_{1x}(x, y) = \pm[k'_{Rx}(x, y) - k'_{Ox}(x, y)], \tag{14}$$

$$k'_{Cy}(x, y) - k'_{1y}(x, y) = \pm[k'_{Ry}(x, y) - k'_{Oy}(x, y)], \tag{15}$$

$$k'_{Cz}(x, y) - k'_{1z}(x, y) = \pm[1/T_e(x, y)][k'_{Rz}(x, y) - k'_{Oz}(x, y)]. \tag{16}$$

Equations (14) and (15) are always satisfied because of the image equations [10].

Generally, aspheric recording or reconstruction wavefronts will be necessary to satisfy simultaneously Eqs. (14), (15), due to the (x, y) dependence. If we want to use spheric and collimated wavefronts, the previous equations are satisfied only approximately. This situation requires that $T_e(x, y)$ remains constant, as it will be shown in Sect. 5, for a holographic lens made in laboratory and we shall prove that this approximation is acceptable.

We shall first assume that the $T_e(x, y)$ function is constant, taking the mean value of the $T_e(x, y)$ function over the entire surface of the HL, $\langle T_e(x, y)\rangle$

$$T_e(x, y) \approx \langle T_e(x, y)\rangle \equiv T_e. \tag{17}$$

Using the equation for the propagation vectors of the light in air at the point of the HL with coordinates $(x, y, z = 0^-)$, $\boldsymbol{k}_q$

$$\boldsymbol{k}_q(x, y) = (2\pi/\lambda_q)(\boldsymbol{r}_q/|\boldsymbol{r}_q|), \tag{18}$$

and using Eq. (9), it is possible to obtain the expression for the propagation vectors in the medium, $\boldsymbol{k}'_q$. Expanding the expression obtained for $\boldsymbol{k}'_q$ into series of powers, we retain terms not higher than the second power, and by substituting the final expression of $\boldsymbol{k}'_q$ into Eqs. (14)–(16) with $T_e(x, y) \approx T_e$ (Eq. (17)) we obtain, for a specified recording geometry, the expressions for the coordinates of the reconstruc-

tion sources needed to fulfil the Bragg condition:

$$\begin{bmatrix} \frac{x_C}{R_C} \\ \frac{x_I}{R_I} \end{bmatrix} = \pm \begin{bmatrix} a & b \\ b & a \end{bmatrix} \begin{bmatrix} \frac{x_R}{R_R} \\ \frac{x_O}{R_O} \end{bmatrix}, \tag{19}$$

$$\begin{bmatrix} \frac{y_C}{R_C} \\ \frac{y_I}{R_I} \end{bmatrix} = \pm \begin{bmatrix} a & b \\ b & a \end{bmatrix} \begin{bmatrix} \frac{y_R}{R_R} \\ \frac{y_O}{R_O} \end{bmatrix}, \tag{20}$$

$$\begin{bmatrix} \frac{1}{R_C} \\ \frac{1}{R_I} \end{bmatrix} = \pm \begin{bmatrix} a & b \\ b & a \end{bmatrix} \begin{bmatrix} \frac{1}{R_R} \\ \frac{1}{R_O} \end{bmatrix}. \tag{21}$$

Similarly, for a specified reconstruction geometry, the required expressions for the coordinates of the recording sources which satisfy Bragg's Law are as follows:

$$\begin{bmatrix} \frac{x_R}{R_R} \\ \frac{x_O}{R_O} \end{bmatrix} = \pm \begin{bmatrix} c & d \\ d & c \end{bmatrix} \begin{bmatrix} \frac{x_C}{R_C} \\ \frac{x_I}{R_I} \end{bmatrix}, \tag{22}$$

$$\begin{bmatrix} \frac{y_R}{R_R} \\ \frac{y_O}{R_O} \end{bmatrix} = \pm \begin{bmatrix} c & d \\ d & c \end{bmatrix} \begin{bmatrix} \frac{y_C}{R_C} \\ \frac{y_I}{R_I} \end{bmatrix}, \tag{23}$$

$$\begin{bmatrix} \frac{1}{R_R} \\ \frac{1}{R_O} \end{bmatrix} = \pm \begin{bmatrix} c & d \\ d & c \end{bmatrix} \begin{bmatrix} \frac{1}{R_C} \\ \frac{1}{R_I} \end{bmatrix}. \tag{24}$$

In the above matrix relations, the parameters a, b, c and d are defined as:

$$a = \frac{1}{2}\left[\frac{N}{T_e} + \mu\right], \qquad b = \frac{1}{2}\left[\frac{N}{T_e} - \mu\right], \tag{25}$$

$$c = \frac{1}{2}\left[\frac{T_e}{N} + \frac{1}{\mu}\right], \qquad d = \frac{1}{2}\left[\frac{T_e}{N} - \frac{1}{\mu}\right]. \tag{26}$$

Expressions (25) and (26) show that if $\mu = T_e/N$, the coordinates of the reconstruction beam depend only on the reference beam coordinates and vice versa, and the same occurs with the image beam and object beam coordinates.

4. Analysis of aberrations

In order to improve the performance of the final holographic lens, it is helpful to know its aberrations. Whenever below we say aberration, we mean the wavefront aberration [11]. Usually if a wavefront aberration is considered, we utilize a reference sphere centered on the Gaussian image point (x_I, y_I, z_I). The relationship between the Φ_C phase of the reconstruction wavefront of wavelength λ_C at the HL and the Φ_I phase of the image wavefront at the HL is given by [11]

$$\Phi_C = \Phi_I \pm (\Phi_O - \Phi_R) \tag{27}$$

where Φ_R and Φ_O are the phases of the object and reference waves, respectively, and the "$\pm$" refers to the positive and negative first diffraction orders from the HL. When the desired Gaussian phase Φ_I^D differs from the actual image phase Φ_I aberrations occur. The wavefront aberration Δ is the difference between the desired image phase Φ_I^D and the actual image phase Φ_I

$$\Delta = \Phi_I - \Phi_I^D. \tag{28}$$

Taking into account Eq. (27), aberrations can be written as

$$\Delta = \Phi_C - \Phi_I^D \pm (\Phi_O - \Phi_R). \tag{29}$$

When the phases Φ_O, Φ_R, Φ_C and Φ_I^D are the phases of spherical waves, their values in the plane of the hologram are

$$\Phi_q(x, y) = (2\pi/\lambda_q)(r_q - R_q). \tag{30}$$

According to Equation (30), the wavefront aberration Δ will be expressed in radians. Usually, the wavefront aberration is expressed in unities of reconstruction wavelengths [10]. In this case, we define the wavefront aberration as $W(x, y)$, where the relation between Δ and W is given by

$$\Delta(x, y) = (2\pi/\lambda_C) W(x, y), \tag{31}$$

and wavefront aberration in wavelengths is $W(x, y)/\lambda_C$. Using Eqs. (29), (30) and (31), $W(x, y)$ is given by

$$W = r_C - r_I \pm \mu(r_O - r_R) - [R_C - R_I \pm \mu(R_O - R_R)]. \tag{32}$$

We take as the measure of the aberrations the root mean square value A, [12], of the wavefront aberration $(1/\lambda_C)W(x, y)$ over the entire pupil of the HL, i.e.,

$$A = \frac{1}{\lambda_C}\left[\frac{\iint W^2(x, y)\,dx\,dy}{\iint dx\,dy}\right]^{1/2} \cong \frac{1}{\lambda_C}\left[\sum_{i=0}^{N}\sum_{j=0}^{N}\frac{W_{ij}^2}{(N+1)^2}\right]^{1/2}. \tag{33}$$

In order to approximate the integral, we use a set of $(N+1)^2$ sample points, where $W_{ij} \equiv W(x_i, y_j)$ is the sample value of $W(x, y)$ in an incremental area $\Delta x \Delta y$ located at point (x_i, y_j) on the HL, with $\Delta x = D_x/N$ and $\Delta y = D_y/N$, D_x and D_y being the dimensions of the HL, and:

$$x_i = \left[i - \frac{N}{2} \right] \Delta x, \quad y_j = \left[j - \frac{N}{2} \right] \Delta y. \tag{34}$$

If the exit pupil of the HL is circular and its diameter is D, we assume $W(x_i, y_j) = 0$ for $x_i^2 + y_j^2 > D^2/4$ in Eq. (33), and we substitute $(N+1)^2$ in the denominator for N', N' being the number of points inside the circle of diameter D.

5. Numerical example and experimental results

The optimization procedure for recording or reconstruction geometry for maximum diffraction efficiency described above is illustrated here for a holographic lens characterized by the following parameters (Fig. 3):

$R_R = \infty$, $\alpha_R = 40°$, $\beta_R = 0°$,

$R_O = -325$ mm, $\alpha_O = 0°$, $\beta_O = 0°$,

$\lambda_R = 633$ nm, $D = 80$ mm,

where D is the diameter of the HL. The HL was fabricated in bleached photographic emulsion Agfa–Gevaert 8E75 HD, using AAC developer and R–9 solvent bleaching [13]. Due to the symmetry of the system with respect to the XZ plane, it is possible to reduce the analysis at that plane.

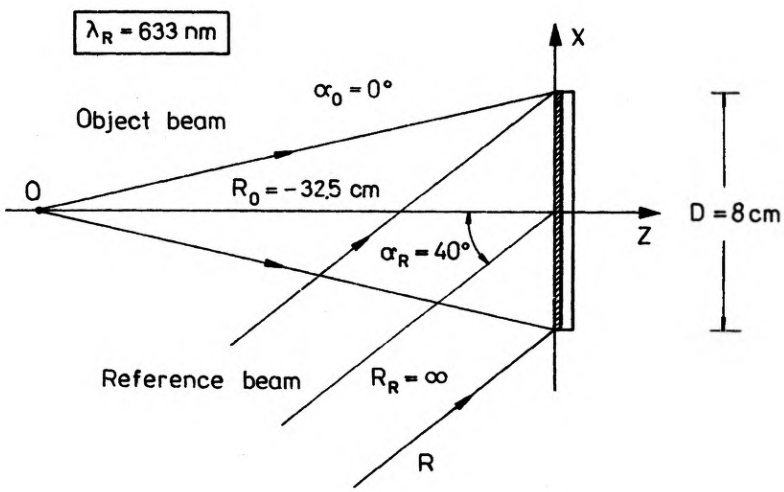

Fig. 3. Diagram of the arrangement used to record the holographic lens analysed in the numerical example. The reference beam is collimated and the object beam divergent

Once the lens is processed, the next step is to find the value of T_e/N. Since at each point of the lens the exposure values, the spatial frequency and the slant angle of the interference fringes are different, the T_e/N parameter will be different as well. Given the symmetrical nature of the HL, we will only determine T_e/N on the X axis

points of the lens. We will show that these measurements are sufficient to obtain acceptable diffraction efficiencies. The same wavelength is used in both reconstruction and recording ($\lambda_C = 633$ nm).

Equation (7) is used to determine $(T_e/N)(x)$. It is modified as necessary according to the local grating of each point of the X axis with μ being 1

$$\frac{T_e}{N}(x) = \frac{\sin\alpha_R(x) + \sin\alpha_O(x)}{2\sin\alpha_C(x) + \sin\alpha_O(x) - \sin\alpha_R(x)}. \tag{35}$$

We have chosen the points ranging from -40 mm to $+40$ mm as the values of x, at 10 mm intervals, and we identified the value of the reconstruction angle that produces maximum diffraction efficiency in each case (Fig. 4). We call this angle $\alpha_C^B(x)$.

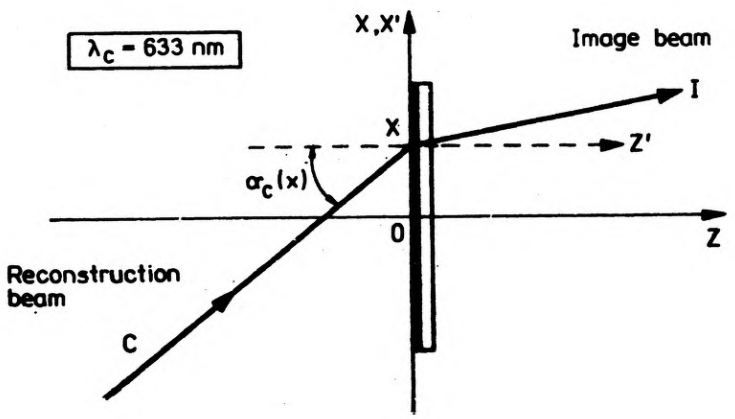

Fig. 4. Diagram of the reconstruction of each "local grating" located on a point of the X axis of the lens in order to find the corresponding Bragg's angle

Figure 5 shows the experimental values for maximum diffraction efficiency and the corresponding reconstruction angles for each point x on the lens.

Knowing the reconstruction angle for maximum diffraction efficiency, it is possible to calculate T_e/N from Eq. (35). In Figure 6 we see the values of $T_e/N(x)$ as well as the average value obtained $\langle T_e/N(x)\rangle = 0.85$.

According to Equations (19)–(21) and assuming that $T_e/N = 0.85$ and $\mu = 1$, the desired reconstruction parameters of high diffraction efficiency are:

$$R_C = -3683 \text{ mm}, \quad \alpha_C = 44.4°, \quad \beta_C = 0°.$$

Figure 7 shows diffraction efficiency as a function of coordinate x for $T_e/N = 1.00$ (identical recording and reconstruction geometries), and $T_e/N = 0.85$ and also shows maximum diffraction efficiency measured experimentally. We can see that using the $T_e/N = 0.85$ reconstruction geometry, approximate maximum diffraction efficiencies can be obtained.

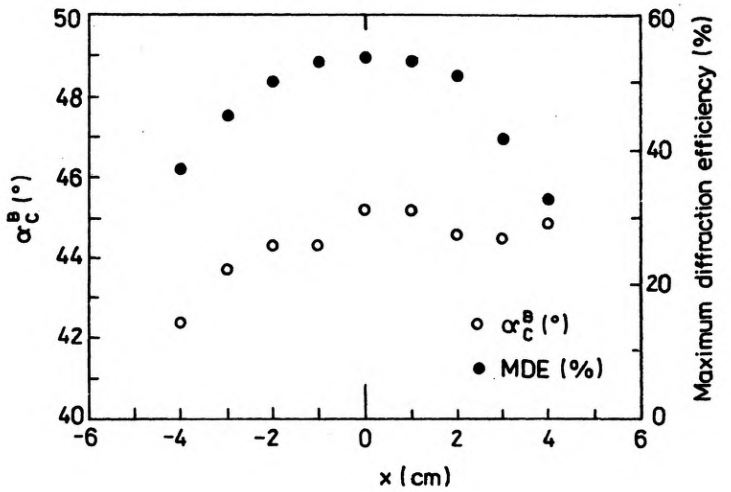

Fig. 5. Maximum diffraction efficiency measured experimentally and the corresponding Bragg's angles as a function of the points on the X axis of the pupil of the holographic lens analysed in the example

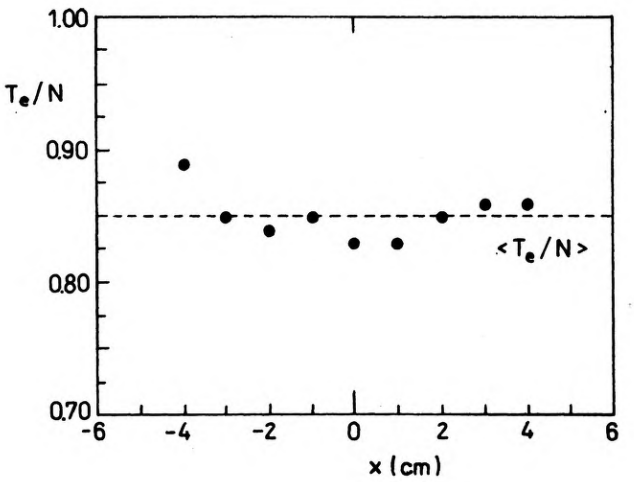

Fig. 6. Values of $T_e/N(x)$ as well as the average value obtained $\langle T_e/N(x)\rangle = 0.85$

In this case, the root mean square value of the wavefront aberration over the entire surface of the holographic lens is $A = 54\lambda_C$.

Once the T_e/N value of the lens being analysed is known, it is possible to use the equation in the opposite direction. In other words, for any given reconstruction

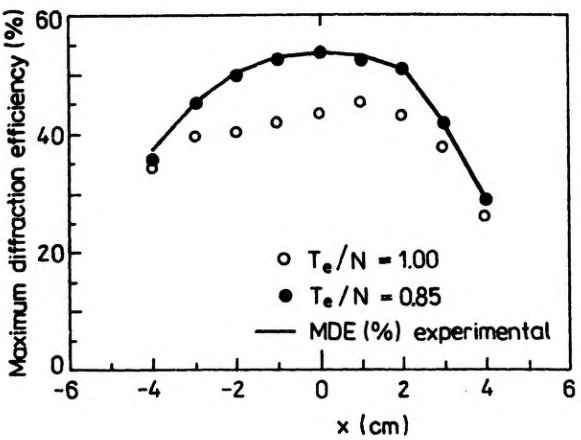

Fig. 7. Diffraction efficiency as a function of the X coordinate for $T_e/N = 1.00$ (identical recording and reconstruction geometries) and $T_e/N = 0.85$ along with the maximum diffraction efficiency measured experimentally

geometry (which does not differ greatly from the recording geometry used in the asymmetric lens studied) we want to be able to find the recording geometry needed if $T_e/N = 0.85$ and $\mu = 1$. If the desired reconstruction geometry is:

$$R_C = \infty, \qquad \alpha_C = 40°, \qquad \beta_C = 0°,$$

$$R_I = -325 \text{ mm}, \qquad \alpha_I = 0°, \qquad \beta_I = 0°,$$

and $T_e/N = 0.85$, from Eqs. (22)–(24), we obtain:

$$R_R = 4333 \text{ mm}, \qquad \alpha_R = 36.5°, \qquad \beta_R = 0°,$$

$$R_O = -351 \text{ mm}, \qquad \alpha_O = -2.8°, \qquad \beta_O = 0°.$$

By choosing recording sources and in spite of the variations that take place in the recording material during processing, we can ensure that during reconstruction with a collimated beam at a 40° angle to the Z axis, the image beam will be divergent, and characterized by the desired characteristics and maximum diffraction efficiency. Nevertheless, aberrations will appear in this beam, just as we pointed out earlier. The root mean square value of the wavefront aberration over the entire surface of the holographic lens is $A = 39\lambda_C$.

6. Discussion and final remarks

Equations (11)–(13) are obtained by applying the hypothesis on local gratings which includes the introduction of the recording material and its processing into the fabrication of holographic lenses. They show the relationship between the vector

of each local grating at one point (x, y) of the lens before and after processing. Included in the equations are both the effective thickness and its relation to the deformations in the recording material. First of all, these equations and the maximum diffraction efficiency equations at the stage of lens reconstruction require that relationships presented in (14)–(16) must be met. These link the wave vectors to the material and are nothing more than Bragg's law applied to each and every local grating on the lens.

As a consequence of these expressions, and when all of the beams used in recording and reconstruction are collimated or spheric wavefronts, new equations can be proposed which relate the different coordinates of the reconstruction and image sources to the object and reference sources and vice versa if Bragg's law is satisfied. Here the most important issue is that in all of these Eqs. (19)–(26) the effective thickness (expressed by T_e), the index quotients (expressed by N) and the wavelength quotients (expressed by μ) are all present. Expressions (19)–(26) offer a set of new possibilities in the area of recording and reconstruction geometries of HLs as a function of the values that can be assigned to the three aforementioned parameters (T_e, N and μ), the application of which was not possible in other geometric models that did not include the variations in recording material due to processing. All this can lead to a study of the influence of these equations on the predesign of holographic lenses.

However, we must take account of the fact that the recording and reconstruction wavelengths are different. In our case, we add the important influence of the recording material and Eqs. (25) and (26), which put parameters T_e, N and μ on equal grounds. Thus, if the right choices are made as regards recording material and processing (T_e and N) as well as recording and reconstruction wavelengths μ, it is possible to find situations in which some aberrations are compensated. In the case we analysed experimentally, it is possible to cancel coma and astigmatism and ensure maximum diffraction efficiency if $\mu = N/T_e$ [4], that is, if the reconstruction wavelength is 745 nm (the value of A in this case is 1.5 λ_C, much lower than those obtained with a reconstruction wavelength of 633 nm).

Finally, it will be possible to obtain techniques for minimizing aberrations using aspheric wavefronts during recording that are obtained from holograms which are computer-generated [9] or by using recursive techniques, that is, using as recording beams wavefronts which come from other holographic lenses [14]. And now there are greater possibilities for success when these techniques are used, because there are more parameters to combine (T_e, N and μ).

References

[1] CLOSE D. H., Opt. Eng. **14** (1975), 408.
[2] AMITAI Y., FRIESEM A. A., Proc. Soc. Photo-Opt. Instrum. Eng. **1136** (1989), 126.
[3] MIKHAILOV I. A., Opt. Spectrosc. **58** (1985), 374.
[4] BELENDEZ A., PASCUAL I., FIMIA A., Proc. Soc. Photo-Opt. Instrum. Eng. **1136** (1989), 58.
[5] KOGELNIK H., Bell. System Tech. J. **48** (1969), 2909.
[6] BELENDEZ A., *Influences of recording material in the holographic optical elements characteristics*, Ph. Degree Thesis, University of Valencia, 1990, Spain.

[7] BELENDEZ A., PASCUAL I., FIMIA A., Proc. Soc. Photo-Opt. Instrum. Eng. **1507** (1991), in press.
[8] OLSON D. W., Am. J. Phys. **57** (1989), 445.
[9] WINICK K. A., J. Opt. Soc. Am. **72** (1982), 143.
[10] LATTA J. N., Appl. Opt. **10** (1971), 599.
[11] CHAMPAGNE E. B., J. Opt. Soc. Am. **57** (1967), 51.
[12] CHEN H., HERSHEY R. R., LEITH E. N., Appl. Opt. **26** (1987), 1983.
[13] CRESPO J., FIMIA A., QUINTANA J. A., Appl. Opt. **25** (1986), 1642.
[14] AMITAI Y., FRIESEM A. A., J. Opt. Soc. Am. A. **5** (1982), 143.

Received June 14, 1991

Оптимизация геометрии реконструкции для максимальной дифракционной эффективности в HOE

Проведен анализ отношения между регистрацией и геометрией реконструкции для получения максимальной дифракционной эффективности в толстых голографических линзах. Даны теоретические выражения с учетом изменчивости регистрирующего материала в зависимости от обработки. Исследовали отдельные голографические линзы как теоретически, так и экспериментально, находя оптимальную геометрию реконструкции для максимума дифракционной эффективности, а также появляющиеся аберрации.

Перевел Станислав Ганцаж